

# Interplanetary Plasma Scattering Diagnostics from Anisotropy-time Profiles of Solar Energetic Particles

R. Schlickeiser<sup>1,\*</sup>, S. Artmann<sup>1</sup> and W. Dröge<sup>2</sup>

<sup>1</sup>*Institut für Theoretische Physik, Lehrstuhl IV: Weltraum-und Astrophysik, Ruhr-Universität Bochum, D-44780 Bochum, Germany*

<sup>2</sup>*Lehrstuhl für Astronomie, Institut für Theoretische Physik und Astrophysik, Universität Würzburg, Am Hubland, D-97074 Würzburg, Germany*

**Abstract:** The anisotropy-time profile of solar particle events provides a powerful diagnostics tool to the interplanetary plasma scattering parameters of energetic charged particles. In the weak focusing limit of the transport of solar particles in axisymmetric MHD turbulence, the particle anisotropy consists of two contributions, the streaming and the Compton-Getting contribution, resulting from the parallel spatial gradient and the momentum gradient of the isotropic part of the particles' phase space density, respectively. These gradients can be calculated from the appropriate solution to the time-dependent focused transport equation of solar particles.

For the illustrative case of the solution of the one-dimensional time-dependent focused transport equation with a constant focusing length and a point-like instantaneous injection of particles the streaming and Compton-Getting contributions to the anisotropy-time profile are analytically calculated in MHD turbulence consisting of isospectral undamped slab Alfvén waves for equal magnetic helicity. The Compton-Getting contribution scales proportional to the ratio of interplanetary Alfvén speed to solar particle speed, and therefore is much smaller than the streaming contribution for the observed mildly relativistic solar particles. After vanishing anisotropy values at times  $t < t_M$  the streaming anisotropy suddenly attains its

maximum value  $A_{S,max} = \frac{3}{2} + \frac{\lambda(p)}{2L}$  at  $t_M = t_0 + (z-z_0)/v$ . At later times the streaming anisotropy decreases  $\propto (t-t_0)^{-1}$

approaching the asymptotic finite value  $(\lambda(p)/2L)$  for  $t-t_0 \rightarrow \infty$ , positive or negative, depending on the sign of the focusing length  $L$ . The new analytical form of the streaming anisotropy provides an excellent fit to the observed anisotropy profiles from the eastern solar particle event of 2001 April 15 for 1.3 GeV protons, but does not well reproduce the anisotropies of 510 keV electrons.

**Keywords:** Cosmic rays, plasma turbulence, diffusion.

## 1. INTRODUCTION

The correct understanding of the interactions between cosmic rays and partially turbulent magnetic fields is one of the fundamental topics of modern plasma astrophysics. The study of energetic solar particle propagation offers a unique possibility to test model predictions with in-situ measurements. Modern in-situ instrumentation routinely provides not only the measurement of interplanetary plasma parameters but also observations with directional information of solar energetic electrons and ions over a wide range of rigidities (for review see [1]). If in these events the large-scale structure of the interplanetary magnetic field is close to the nominal Archimedean spiral, and if the event is not disturbed by interplanetary shocks and coronal mass ejections, the measured intensity-time and anisotropy-time profiles of solar energetic particles are very adequate to test the predictions of idealized solar particle transport theories. Here the anisotropy is defined as  $A(z,p,t) = 3S(z,p,t)/vN(z,p,t)$  as the ratio of the streaming  $S$  to the differential number density  $N$  of the particles. In terms of the phase space density of particles per

magnetic line length  $f_0$  the anisotropy equals three times the ratio of first to zeroth moment with respect to the pitch-angle  $\mu$ :

$$A(z,p,t) = 3 \frac{\int_{-1}^1 d\mu, \mu f_o(z,p,\mu,t)}{\int_{-1}^1 d\mu, f_o(z,p,\mu,t)} \quad (1)$$

It is the purpose of this work to calculate the anisotropy (1) as a function of time from the recent solution of the solar particle focused transport equation in the weak focusing limit (Schlickeiser and Shalchi [2] – hereafter referred to as SS08). We demonstrate that the comparison with observed anisotropy-time profiles from solar particle events provides powerful diagnostics of the scattering conditions of energetic particles in the interplanetary plasma. For the case of pointlike instantaneous injection of particles, the anisotropy-time profile immediately yields both, the ratio  $\lambda/L$  of the parallel scattering mean free path to the focusing length, and the distance  $z - z_0$  along the guide magnetic field to the origin of the solar event.

## 2. Basic Equations

The transport of cosmic ray particles in the partially turbulent interplanetary electromagnetic fields is described by

\*Address correspondence to this author at the Institut für Theoretische Physik, Lehrstuhl IV: Weltraum-und Astrophysik, Ruhr-Universität Bochum, D-44780 Bochum, Germany; E-mail: rsch@tp4.rub.de

a Fokker-Planck approach with a dominating guide magnetic field with superposed electric and magnetic fluctuations. The spatially varying guide magnetic field with the focusing length  $L^{-1} = -d \ln(B_0(z))/dz$  gives rise to the additional adiabatic focusing term [3-6] in the Fokker-Planck transport equation for the gyrotropic cosmic ray phase space density per magnetic line length  $f_0(X, Y, z, p, \mu, t)$ . The interplanetary plasma turbulence consists predominantly of magnetohydrodynamic (MHD) turbulence well below the nonrelativistic electron gyrofrequency, whose fluctuating electric fields are much smaller than the fluctuating magnetic fields ( $\delta E \ll \delta B$ ). In this case the gyrotropic phase space distribution function  $f_0(X, Y, z, p, \mu, t)$  due to dominating pitch-angle diffusion adjusts very quickly to a quasi-equilibrium which is close to the isotropic equilibrium distribution  $F_0(X, Y, z, p, t)$  [7-10], where  $X$  and  $Y$  denote the perpendicular guiding center coordinates of the cosmic ray particle,  $z$  is the spatial coordinate parallel to  $\underline{B}_0$  and  $\mu = \cos \theta$  its pitch-angle cosine with respect to  $\underline{B}_0$ . According to the diffusion approximation  $|g_0| \ll F_0$  one finds

$$f_0(X, Y, z, p, \mu, t) = F_0(X, Y, z, p, t) + g_0(X, Y, z, p, \mu, t) \quad (2)$$

with the isotropic part

$$F_0(X, Y, z, p, t) = \frac{1}{2} \int_{-1}^1 d\mu f_0(X, Y, z, p, \mu, t) \quad (3)$$

and the cosmic ray anisotropy  $g_0 = f_0 - F_0$  fulfilling

$$\int_{-1}^1 d\mu g_0(X, Y, z, p, \mu, t) = 0 \quad (4)$$

SS08 have shown that the cosmic ray anisotropy in axisymmetric MHD turbulence in the weak focusing limit (scattering length  $\lambda \ll L$ ) consists of two parts

$$g_0(X, Y, z, p, \mu, t) = g_s(z, p, \mu, t) + g_{CG}(z, p, \mu, t) \quad (5)$$

with the streaming anisotropy ( $v$  denotes the cosmic ray particle velocity)

$$g_s(z, p, \mu, t) = \left[ \int_{-1}^1 d\mu \frac{(1-\mu)(1-\mu^2)}{D_{\mu\mu}(\mu)} - 2 \int_{-1}^{\mu} dx \frac{1-x^2}{D_{\mu\mu}(x)} \right] \frac{v}{4} \frac{\partial F_0}{\partial z} \quad (6)$$

caused by the parallel spatial gradient of the isotropic part of the phase space density, and the Compton-Getting contribution

$$g_{CG}(z, p, \mu, t) = \left[ \int_{-1}^1 d\mu \frac{(1-\mu)D_{\mu p}(\mu)}{D_{\mu\mu}(\mu)} - 2 \int_{-1}^{\mu} dx \frac{D_{\mu p}(x)}{D_{\mu\mu}(x)} \right] \frac{1}{2} \frac{\partial F_0}{\partial p} \quad (7)$$

In Eqs. (6) and (7)  $D_{\mu\mu}(\mu)$  and  $D_{\mu p}(\mu)$  denote the two largest Fokker-Planck coefficients describing resonant and/or nonresonant interactions of cosmic ray particles with the MHD turbulence.

## 2.1. Anisotropy

Using Eqs. (2) – (5) we obtain for the anisotropy (1)

$$A(z, p, t) = \frac{3}{2F_0} \int_{-1}^1 d\mu \mu g_0(z, p, \mu, t) = A_s(z, p, t) + A_{CG}(z, p, t) \quad (8)$$

with the streaming contribution

$$A_s(z, p, t) = \frac{3v}{8} \frac{\partial \ln F_0}{\partial z} \int_{-1}^1 d\mu \mu \left[ \int_{-1}^1 dx \frac{(1-x)(1-x^2)}{D_{\mu\mu}(x)} - 2 \int_{-1}^{\mu} dx \frac{1-x^2}{D_{\mu\mu}(x)} \right] \quad (9)$$

$$= - \int_{-1}^1 d\mu \frac{(1-\mu^2)^2}{D_{\mu\mu}(\mu)} \frac{3v}{8} \frac{\partial \ln F_0}{\partial z} = \frac{3\kappa_{zz}(z, p)}{v} \frac{\partial \ln F_0}{\partial z} = -\lambda \frac{\partial \ln F_0}{\partial z}$$

where

$$\kappa_{zz}(z, p) = \frac{v}{3} \lambda(z, p) = \frac{v^2}{8} \int_{-1}^1 d\mu \frac{(1-\mu^2)^2}{D_{\mu\mu}(\mu)} \quad (10)$$

is the parallel spatial diffusion coefficient, and the Compton-Getting contribution

$$A_{CG}(z, p, t) = \frac{3}{4} \frac{\partial \ln F_0}{\partial p} \int_{-1}^1 d\mu \mu \left[ \int_{-1}^1 dx \frac{(1-x)D_{\mu p}(x)}{D_{\mu\mu}(x)} - 2 \int_{-1}^{\mu} dx \frac{D_{\mu p}(x)}{D_{\mu\mu}(x)} \right] \quad (11)$$

$$= -\frac{3a_{11}}{4} \frac{\partial \ln F}{\partial p},$$

with the rate of adiabatic deceleration

$$a_{11} = \int_{-1}^1 d\mu \frac{(1-\mu^2)D_{\mu p}(\mu)}{D_{\mu\mu}(\mu)} \quad (12)$$

## 2.2. Isospectral Undamped Slab Alfvénic Turbulence

In isospectral undamped slab Alfvénic turbulence the rate of adiabatic deceleration is given by [11]

$$a_{11} = \frac{4V_A}{3v} p H(H_c, \sigma^\pm) \quad (13)$$

where the function

$$H(H_c, \sigma^\pm) = \frac{(1+H_c)^2(1-(\sigma^\pm)^2) - (1-H_c)^2(1-(\sigma^\mp)^2)}{(1+H_c)^2(1-(\sigma^\pm)^2) + (1-H_c)^2(1-(\sigma^\mp)^2)2(1-H_c^2)(1-\sigma^+\sigma^-)} \quad (14)$$

with values between  $-1 \leq H \leq 1$  depends on the magnetic ( $\sigma^\pm$ ) and cross ( $H_c$ ) helicity values.

For equal polarisation states of forward and backward moving waves ( $\sigma^+ = \sigma^- = \sigma$ ) the function (14) simplifies to  $H(H_c, \sigma) = H_c$ , yielding with Eq. (13) for the Compton-Getting contribution (11)

$$A_{CG}(z, p, t) = -\frac{V_A H_c}{v} \frac{\partial \ln F_0}{\partial \ln p} \quad (15)$$

The total anisotropy (8) in axisymmetric MHD turbulence then in general is

$$A(z, p, t) = A_s(z, p, t) + A_{CG}(z, p, t) = -\lambda \frac{\partial \ln F_0}{\partial z} - \frac{V_A H_c}{v} \frac{\partial \ln F_0}{\partial \ln p} \quad (16)$$

which holds for any isotropic phase space density  $F_0(z, p, t)$ . Two remarks have to be made:

- 1) Both contributions to the anisotropy are smaller than unity. While the streaming anisotropy is of order  $\mathcal{O}(\lambda/Z) < 1$ , where  $Z \simeq |L|$  denotes a characteristic spatial scale of the isotropic distribution  $F_0$ , the Compton-Getting contribution is of order  $\mathcal{O}(V_A/v) \ll 1$ . The measured solar energetic particles are so energetic that their individual speeds  $v$  are much larger than the interplanetary Alfvén speed  $V_A$ . Therefore for most solar particle events, where  $\lambda/L \simeq \mathcal{O}(0.1)$ , the streaming anisotropy contribution will dominate the total anisotropy (16).
- 2) For specific physical conditions the transport equation for the isotropic phase space density  $F_0(z, p, t)$  can be solved analytically. For such special cases it is possible to reduce the streaming and Compton-Getting anisotropies further. Below we will use one special solution as an illustrative

example. In future work, we will use additional analytical solutions for spatially varying focusing lengths and finite injection time profiles to investigate the influence of these effects on the anisotropy.

### 2.3. Isotropic Phase Space Density $F_0(z,p,t)$

SS08 demonstrated that the isotropic part of the phase space density  $F_0$  itself evolves according to the one-dimensional time-dependent focused transport equation

$$\begin{aligned} \frac{\partial F_0}{\partial t} - \frac{\partial}{\partial z} \left[ \kappa_{zz}(z,p) \frac{\partial F_0}{\partial z} \right] - \left[ \frac{\kappa_{zz}(z,p)}{L(z)} - \frac{1}{4p^2} \frac{\partial}{\partial p} (vp^2 a_{11}) \right] \\ \frac{\partial F_0}{\partial z} - \frac{va_{11}}{4L(z)} \frac{\partial F_0}{\partial p} = S_0(z,p,t) \end{aligned} \quad (17)$$

which for isospectral undamped slab Alfvénic turbulence upon insertion of Eq. (13) for  $a_{11}$  and  $H(H_c, \sigma) = H_c$  reads

$$\begin{aligned} \frac{\partial F_0}{\partial t} - \frac{\partial}{\partial z} \left[ \kappa_{zz}(z,p) \frac{\partial F_0}{\partial z} \right] - \left[ \frac{\kappa_{zz}(z,p)}{L(z)} - V_A H_c \right] \\ \frac{\partial F_0}{\partial z} + \frac{V_A H_c}{3L(z)} p \frac{\partial F_0}{\partial p} = S_0(z,p,t) \end{aligned} \quad (18)$$

In its simplest form for a spatially constant parallel spatial diffusion coefficient  $\kappa_{zz}(z,p) = \kappa(p)$ , a constant focusing length  $L(z) = L = \text{const.}$ , and negligible  $a_{11}$  the one-dimensional time-dependent focused transport equation then becomes

$$\frac{\partial F_0}{\partial t} - \kappa(p) \frac{\partial^2 F_0}{\partial z^2} - \frac{\kappa(p)}{L} \frac{\partial F_0}{\partial z} = S_0(z,p,t) \quad (19)$$

The solution of Eq. (19) in an infinite medium for the adopted source term  $S_0(z,p,t) = S_1(p) \delta(z-z_0) \delta(t-t_0)$  is given by ( $T = t - t_0$  and  $x = z - z_0$ )

$$F_0(x,p,T \geq 0, L) = \frac{S_1(p)}{2\sqrt{\pi\kappa(p)T}} \exp \left[ - \frac{\left( x + \frac{\kappa(p)T}{L} \right)^2}{4\kappa(p)T} \right] \quad (20)$$

The solution (20) readily yields the gradients  $\partial F_0/\partial z$  and  $\partial F_0/\partial p$  that determine the streaming (3) and Compton-Getting (5) anisotropies.

## 3. ANISOTROPY FOR CONSTANT FOCUSING LENGTH AND INSTANTANEOUS POINTLIKE-INJECTION

### 3.1. Streaming Anisotropy

From the solution (20) we infer

$$\frac{\partial \ln F_0}{\partial z} = \frac{\partial \ln F_0}{\partial x} = - \frac{x + \frac{\kappa(p)T}{L}}{2\kappa(p)T} = - \left[ \frac{z - z_0}{2\kappa(p)T} + \frac{1}{2L} \right] \quad (21)$$

so that the streaming anisotropy (9) becomes

$$A_s(z,p,t) = \frac{\lambda(p)(z - z_0)}{2\kappa(p)(t - t_0)} + \frac{\lambda(p)}{2L} = \frac{3}{2} \frac{(z - z_0)}{v(t - t_0)} + \frac{\lambda(p)}{2L} \quad (22)$$

Describing cosmic ray transport by time-dependent Fokker-Planck and focused diffusion transport equations neglects the finite propagation speed ( $v \leq c$ ) of cosmic ray

particles. Therefore, to describe phenomena at short times after injection a telegrapher-type equation, considered by e.g. [12-15], would be more appropriate. Therefore, the solution (20) is only valid for

$$z - z_0 \leq v(t - t_0) \quad (23)$$

which we accommodate by an appropriate Heaviside function  $\Theta$  in  $(t - t_0)$ , yielding

$$A_s(z,p,t) = \left[ \frac{3}{2} \frac{(z - z_0)}{v(t - t_0)} + \frac{\lambda(p)}{2L} \right] \Theta \left[ (t - t_0) - \frac{z - z_0}{v} \right] \quad (24)$$

For infinitely large focusing length  $|L| \rightarrow \infty$  the streaming anisotropy agrees with the standard pure diffusion behaviour (Fisk and Axford 1969); the inclusion of a finite focusing length obviously provides a finite value of the streaming anisotropy at late times. In Fig. (1) we show the time variation of the streaming anisotropy. After vanishing anisotropy values at times  $t - t_0 < (z - z_0)/v$  the streaming anisotropy suddenly attains its maximum value

$$A_{S,\max} = \frac{3}{2} + \frac{\lambda(p)}{2L} \quad (25)$$

at  $t_M = t_0 + (z - z_0)/v$ . At later times the streaming anisotropy decreases  $\propto (t - t_0)^{-1}$  approaching the asymptotic finite value  $(\lambda(p)/2L)$  for  $t - t_0 \rightarrow \infty$ , positive or negative depending on the sign of the focusing length  $L$ .

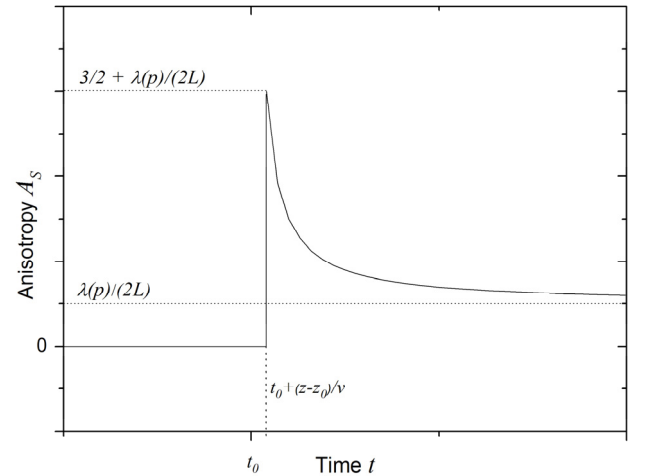


Fig. (1). Streaming anisotropy as a function of time  $t$  for instantaneous injection at time  $t_0$ .

### 3.2. Compton-Getting Anisotropy

From the solution (20) we infer the momentum gradient

$$\frac{\partial \ln F_0}{\partial \ln p} = p \frac{\partial \ln F_0}{\partial p} = \frac{d \ln S_1(p)}{d \ln p} - \frac{1}{4} \frac{d \ln \kappa(p)}{d \ln p} \left[ 2 - \frac{x^2}{\kappa(p)T} + \frac{\kappa(p)T}{L^2} \right] \quad (26)$$

implying for the Compton-Getting anisotropy (15)

$$\begin{aligned} A_{CG}(z,p,t) = \frac{V_A H_c}{v} \left[ \frac{1}{4} \frac{d \ln \kappa(p)}{d \ln p} \left( 2 - \frac{x^2}{\kappa(p)(t - t_0)} + \frac{\kappa(p)(t - t_0)}{L^2} \right) - \frac{d \ln S_1(p)}{d \ln p} \right] \\ \times \Theta \left[ (t - t_0) - \frac{z - z_0}{v} \right] \end{aligned} \quad (27)$$

where we also used the causality condition (23). Observations of interplanetary solar cosmic rays often indicate the power law dependences  $\kappa(p) = k_0 p^\eta$  and  $S_1(p) \propto p^{-\alpha}$ , respectively.

Taking these momentum dependences as illustrative example we obtain

$$A_{CG}(z, p, t) = \frac{V_A H_c}{4v} [4\alpha + 2\eta + \eta G(T)] \Theta \left[ T - \frac{x}{v} \right] \quad (28)$$

with the monotonically increasing function

$$G(T) = \frac{\kappa(p)T}{L^2} - \frac{x^2}{\kappa(p)T} \quad (29)$$

Figs. (2) and (3) show the Compton-Getting anisotropy for  $\alpha = 5$  and  $\eta = 0.5$  for positive ( $H_c > 0$ ) and negative ( $H_c < 0$ ) cross helicity values, respectively.

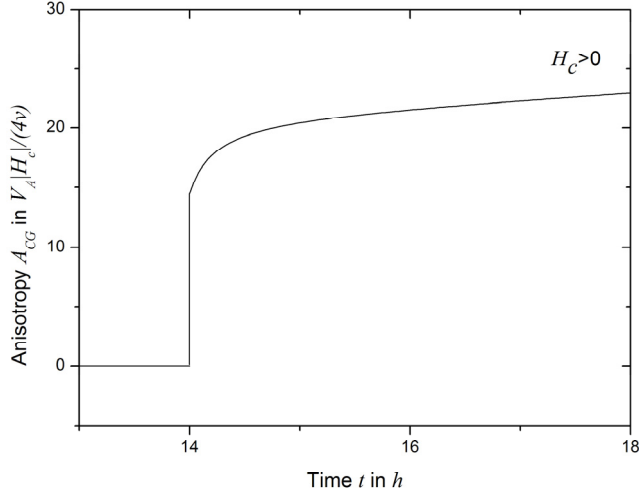


**Fig. (2).** Compton-Getting anisotropy as a function of time  $t$  for instantaneous injection at time  $t_0$  and positive cross helicity values  $H_c > 0$  calculated for the best fit proton parameters of the easter solar particle event of 2001 April 15 and  $x/L = 1.825$ .

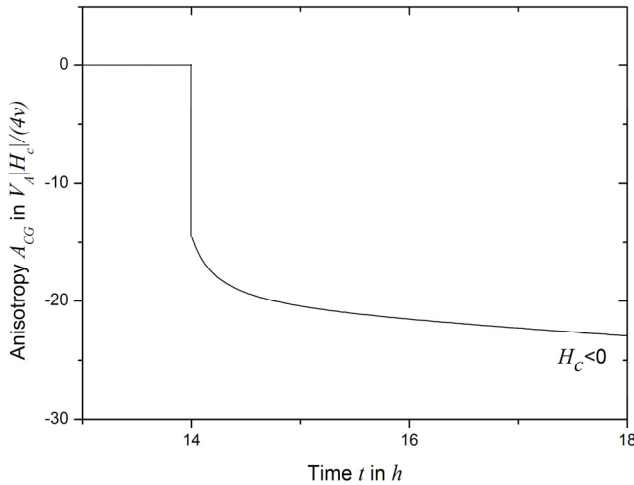


**Fig. (3).** Compton-Getting anisotropy as a function of time  $t$  for instantaneous injection at time  $t_0$  and negative cross helicity values  $H_c < 0$  calculated for the best fit proton parameters of the easter solar particle event of 2001 April 15 and  $x/L = 1.825$ .

For positive cross helicity values, after vanishing anisotropy values at times  $T < x/v$ , the Compton-Getting anisotropy is positive and continuously increases from its minimum value

$$\begin{aligned} A_{CG, H_c > 0, \min} &= \frac{V_A H_c}{4v} \left[ 4\alpha + 2\eta - \eta \frac{xv}{\kappa} \left( 1 - \frac{\kappa^2}{v^2 L^2} \right) \right] \\ &= \frac{V_A H_c}{4v} \left[ 4\alpha + 2\eta - \frac{3\eta x}{\lambda} \left( 1 - \left( \frac{\lambda}{3L} \right)^2 \right) \right] \end{aligned} \quad (30)$$

at  $T_M = x/v$ . For negative cross helicity values, after vanishing anisotropy values at times  $T < x/v$ , the Compton-Getting anisotropy is negative and continuously decreases from its maximum value

$$\begin{aligned} A_{CG, H_c < 0, \max} &= \frac{V_A H_c}{4v} \left[ 4\alpha + 2\eta - \eta \frac{xv}{\kappa} \left( 1 - \frac{\kappa^2}{v^2 L^2} \right) \right] \\ &= \frac{V_A H_c}{4v} \left[ 4\alpha + 2\eta - \frac{3\eta x}{\lambda} \left( 1 - \left( \frac{\lambda}{3L} \right)^2 \right) \right] \end{aligned} \quad (31)$$

at  $T_M = x/v$ . However, as noted before, its values being of order  $\mathcal{O}(V_A/v) \ll 1$  are much smaller than the streaming anisotropy, so it practically does not contribute to the anisotropy of energetic solar particles. For very late times ( $T \gg T_L, T_L = 3(|L|/\lambda)T_M$ ) the Compton-Getting anisotropy

$$A_{CG}(T \gg T_L) \simeq \frac{V_A H_c \eta \kappa}{4v L^2} T \quad (32)$$

formally outnumbers the late streaming anisotropy. However, at these times the solar event intensities have dropped to such small values that meaningful observations cannot be taken.

#### 4. APPLICATION TO THE EASTER SOLAR PARTICLE EVENT OF 2001 APRIL 15

An exceptionally large solar particle event occurred on 2001 April 15 which was associated with a solar flare located at S20 W85 which produced an X14.4 soft X-ray event, type III radio emission and a coronal mass ejection. Fig. (4) shows the anisotropy observations of 1.3 GeV protons by the spaceship Earth neutron monitor network [16] in comparison with the best-fit streaming anisotropy. The anisotropy observations of 510 keV electrons measured with the Wind 3DP instrument [17] are shown in Fig. (5).

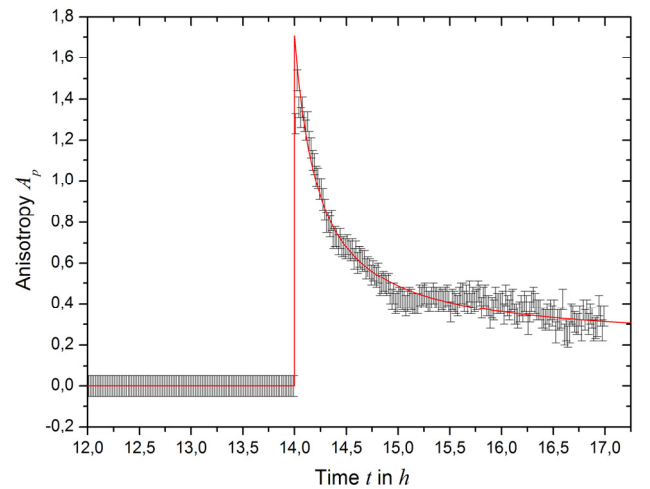


**Fig. (4).** Best fit of the streaming anisotropy to the proton anisotropy observations of the easter solar particle event of 2001 April 15.

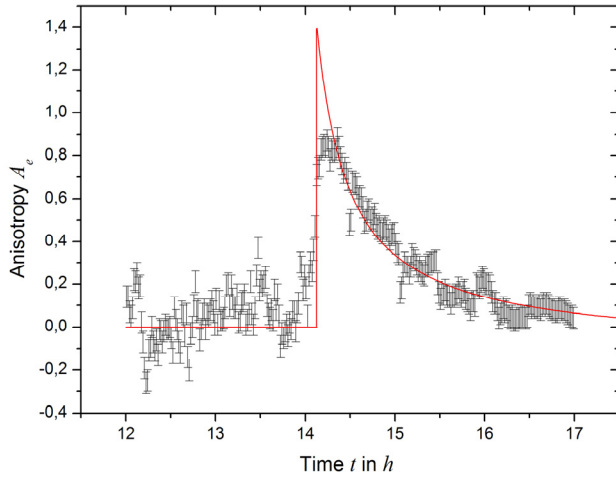


**Fig. (5).** Best fit of the streaming anisotropy to the electron anisotropy observations of the easter solar particle event of 2001 April 15.

In both cases the velocities  $v$  of the cosmic ray particles are known. With

$$\frac{v}{c} = \left[ 1 - \left( 1 + \frac{E_{kin}}{mc^2} \right)^{-2} \right]^{1/2} \quad (33)$$

we find for the protons ( $E_{kin} = 1.3$  GeV) that  $v_p = 0.91c$  and for the electrons ( $E_{kin} = 0.51$  MeV) that  $v_e = 0.87c$ . With a typical interplanetary Alfvén speed  $V_A/c \simeq 3 \cdot 10^{-4}$  the minimum and maximum electron and proton Compton-Getting anisotropies (30) and (31) are thus of order much smaller than the streaming anisotropy.

$$(A_{GC}) \simeq \frac{21H_c V_A}{4v} \simeq 1.8 \cdot 10^{-3} H_c, \quad (34)$$

The streaming anisotropy (24) then is determined by only two free parameters: the distance along the magnetic field line from the flares origin  $x = z - z_0$  and the ratio  $r_{p,e} = \lambda_{p,e}/L$  of the parallel scattering length  $\lambda_{p,e}$  of protons and electrons, respectively, to the focusing length  $L$ . In this case the proton and electron anisotropies are

$$A_p(x, t) = \left[ \frac{1.65x}{cT} + 0.5r_p \right] \Theta \left[ T - \frac{1.10x}{c} \right], \quad (35)$$

$$A_e(x, t) = \left[ \frac{1.72x}{cT} + 0.5r_p \right] \Theta \left[ T - \frac{1.15x}{c} \right]$$

In order to perform a  $\chi^2$ -test we adopt a systematic error of  $\pm 0.05$  to any individual anisotropy measurement. In Fig. (4) and Fig. (5) we show the best fits to the proton and electron observations, whereas Figs. (6) and (7) show the 68- and 90-percent confidence limits on the free parameters.

For protons the best fit is obtained for  $r_p = 0.412$ , and  $x_p = 753c \cdot s = 1.506$  AU yielding a reduced  $\chi_{min,p,df}^2 = 1.01$ . With 90-percent confidence the two parameters are  $r_p = 0.412 \pm 0.040$  and  $x_p = 1.506 \pm 0.150$  AU. The proton observations are extremely well reproduced by our model. The smallness of the ratio  $r_p$  with respect to unity is consistent with the weak focusing limit that the particles' mean free path is smaller than the absolute value of the focusing length. The fit of the intensity-time profile of 1.3 GeV protons [1] gave a value of

$\lambda_p = 0.34$  AU so that we infer for the focusing length  $L = \lambda_p/r_p = 0.825 \pm 0.081$  AU.

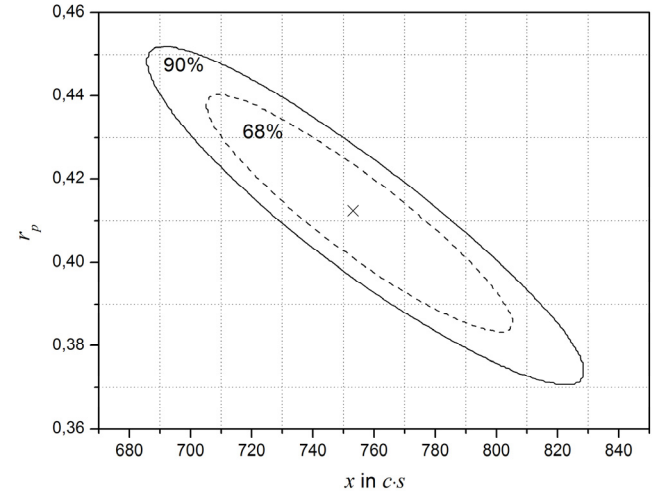


**Fig. (6).** 68- and 90-percent confidence limits for the parameters  $r_p$  and  $x$ .

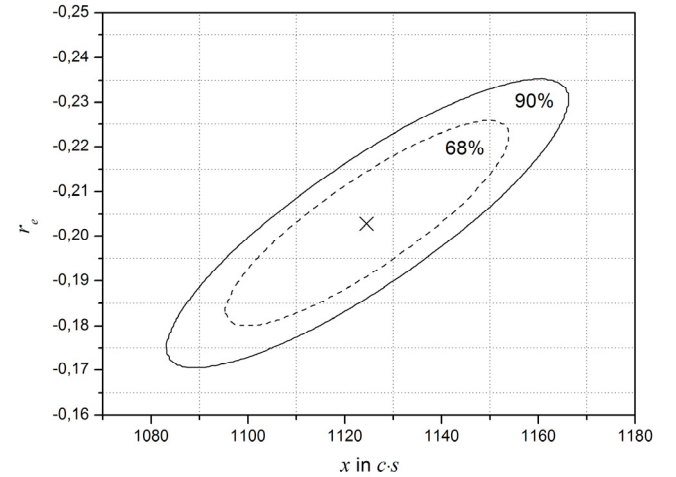


**Fig. (7).** 68- and 90-percent confidence limits for the parameters  $r_e$  and  $x$ .

In contrast, the fit to the electron anisotropies in Fig. (5) is rather poor, also reflected in the large value of the reduced  $\chi_{min,p,df}^2 = 6.13$  for the best fit for  $r_e = -0.203$ , and  $x_e = 1124c \cdot s = 2.248$  AU. Formally, the 90-percent confidence intervals for the two parameter are  $r_e = -0.203 \pm 0.033$  and  $x_e = 2.248 \pm 0.082$  AU. The maximum observed electron anisotropy is far below the theoretically predicted, and implies a negative value of the parameter  $r_e$  pointing to a negative focusing length. The only physical explanation of the negative  $r_e$  would be that the energetic electrons and protons have propagated along different magnetic flux tubes from the flares' point of origin. The electrons propagated a longer path along a converging guide magnetic field (with a negative value of the focusing length  $L$ ), whereas the protons propagated a shorter path along a diverging guide magnetic field (with a positive value of the focusing length). However, this interpretation is unlikely, given the nearly identical observed onset times of the proton and electron events.

We rather conclude from the poor fit to the electron observations that one or several of the underlying

assumptions of our anisotropy model (spatially pointlike and instantaneous injection, particle-wave interaction solely by isospectral undamped slab Alfvén waves, equal magnetic helicity) do not hold for the 510 keV electrons. The smallness of the ratio  $|r_e|$  with respect to unity is consistent with the weak focusing limit so that the diffusion equation still seems to be applicable for the electron transport. However, it is well known [18, 19] that mildly relativistic electrons predominantly resonantly interact with the right-hand circularly polarized Whistler waves and not with Alfvén waves. The higher phase speed of Whistler waves might lead to a much larger value of the rate of adiabatic deceleration  $a_{11}$  for electrons, and so to a larger negative Compton-Getting contribution. Before inspecting these likely modifications we will not further interpret our electron fit results. However, positively seen, this discovered discrepancy emphasizes the diagnostics power of anisotropy-time profiles of different solar particle species.

## 5. SUMMARY AND CONCLUSIONS

We demonstrate that the anisotropy-time profile of solar particle events provides a powerful diagnostics tool to the interplanetary plasma scattering parameters of energetic charged particles. In the weak focusing limit of the transport of solar particles in axisymmetric MHD turbulence, the particle anisotropy, defined as the ratio of the streaming to the differential number density of particles, is given by two contributions, the streaming and the Compton-Getting contribution, resulting from the parallel spatial gradient and the momentum gradient of the isotropic part of the particles' phase space density, respectively. These gradients can be calculated from the appropriate solution to the time-dependent focused transport equation of solar particles.

For the illustrative case of the solution of the one-dimensional time-dependent focused transport equation with a constant focusing length and a point-like instantaneous injection of particles the streaming and Compton-Getting contributions to the anisotropy-time profile are analytically calculated in MHD turbulence consisting of isospectral undamped slab Alfvén waves for equal magnetic helicity. Then the streaming anisotropy is of order  $\mathcal{O}(\lambda/Z) < 1$ , where  $Z \simeq |L|$  denotes a characteristic spatial scale of the isotropic distribution  $F_0$ . It is demonstrated that the Compton-Getting contribution scales proportional to the ratio of interplanetary Alfvén speed to solar particle speed. The observed solar particles are so energetic that their individual speeds  $v$  are much larger than the interplanetary Alfvén speed  $V_A$ . Therefore for most solar particle events, where  $\lambda/L \simeq \mathcal{O}(0.1)$ , the streaming anisotropy contribution dominates the total anisotropy, at least at times before the solar event intensities have dropped to such small values that meaningful observations cannot be taken.

It is shown that the streaming anisotropy contribution agrees with the standard pure diffusion behaviour for infinitely large focusing length. After vanishing anisotropy values at times  $t < t_M$  the streaming anisotropy suddenly attains its maximum value  $A_{S,\max} = \frac{3}{2} + \frac{\lambda(p)}{2L}$  at  $t_M = t_0 + (z - z_0)/v$ . At later times the streaming anisotropy decreases  $\propto (t - t_0)^{-1}$  approaching the asymptotic finite value  $(\lambda(p)/2L)$  for  $t - t_0 \rightarrow \infty$ ,

positive or negative depending on the sign of the focusing length  $L$ . The Compton-Getting anisotropy contribution has a different temporal behaviour. For positive (negative) cross helicity values, after vanishing anisotropy values at times  $t < t_M$ , the Compton-Getting anisotropy is positive (negative) and continuously increases (decreases) from its minimum (maximum) value. For very late times  $t \gg t_L = 3(|L|/\lambda)t_M$  the Compton-Getting anisotropy formally outnumbers the late streaming anisotropy. However, as noted, at these times the solar event intensities have dropped to such small values that meaningful observations cannot be taken.

The analytical form of the streaming anisotropy provides an excellent fit to the observed anisotropy profiles from the easter solar particle event of 2001 April 15 for 1.3 GeV protons. With 90 percent confidence we obtain for the ratios of mean free path to focusing length for protons  $r_p = 0.412 \pm 0.040$ . The observed anisotropies of 510 keV electrons from the same event are not well reproduced by our model, indicating that one or several of the underlying assumptions of our anisotropy model (spatially pointlike and instantaneous injection, particle-wave interaction solely by isospectral undamped slab Alfvén waves, equal magnetic helicity), do hold for the 1.3 GeV protons, but not for the 510 keV electrons.

## ACKNOWLEDGEMENT

Partially supported by the Deutsche Forschungsgemeinschaft through the grants Schl 201/19-1 and Schl 201/21-1 is gratefully acknowledged.

## REFERENCES

- [1] Dröge W. Probing heliospheric diffusion coefficients with solar energetic particles. *Adv Space Res* 2005; 35: 532-42.
- [2] Schlickeiser R, Shalchi A. Cosmic-ray diffusion approximation with weak adiabatic focusing. *Astrophys J* 2008; 686: 292-302 (SS08).
- [3] Kulsrud R, Pearce WP. The effect of wave-particle interactions on the propagation of cosmic rays. *Astrophys J* 1969; 156: 445-69.
- [4] Roelof EC. Propagation of solar cosmic rays in the interplanetary magnetic field, In: Ögelman H, Wayland JR, Eds. *Lectures in high energy astrophysics*, Scientific and Technical Information Division, Office of Technology Utilization, NASA: Washington, DC 1969; pp. 111.
- [5] Earl JA. The effect of adiabatic focusing upon charged-particle propagation in random magnetic fields. *Astrophys J* 1976; 205: 900-19.
- [6] Kunstmann JA. new transport mode for energetic charged particles in magnetic fluctuations superposed on a diverging mean field. *Astrophys J* 1979; 229: 812-20.
- [7] Jokipii JR. Cosmic-Ray Propagation. I. Charged particles in a random magnetic field. *Astrophys J* 1966; 146: 480-7.
- [8] Hasselmann K, Wibberenz G. Scattering of charged particles by random electromagnetic fields. *Zeitschrift für Geophysik* 1968; 34: 353-88.
- [9] Skilling J. Cosmic ray streaming. I - Effect of Alfvén waves on particles. *Monthly Not Roy Astron Soc* 1975; 172: 557-66.
- [10] Schlickeiser R. Cosmic-ray transport and acceleration. I - Derivation of the kinetic equation and application to cosmic rays in static cold media. *Astrophys J* 1989; 336: 243-63.
- [11] Dung R, Schlickeiser R. The influence of the Alfvénic cross and magnetic helicity on the cosmic ray transport equation. I - Isospectral slab turbulence. *Astron Astrophys* 1990; 240: 537-40.
- [12] Fisk LA, Axford WI. Anisotropies of solar cosmic rays. *Solar Phys* 1969; 7: 486-98.
- [13] Gombosi TJ, Jokipii JR, Kota J, Lorencz K, Williams LL. The telegraph equation in charged particle transport. *Astrophys J* 1993; 403: 377-84.

- [14] Lu JY, Zank GP, Rankin R, Marchand R. The transport of charged particles in a flowing medium. *Astrophys J* 2002; 576: 574-86.
- [15] Fedorov YI, Shakhov BA. Description of non-diffusive solar cosmic ray propagation in a homogeneous regular magnetic field. *Astron Astrophys* 2003; 402: 805-817.
- [16] Bieber JW, Evenson P, Dröge W, *et al.* Spaceship earth observations of the easter 2001 solar particle event. *Astrophys J* 2004; 601: L103-L106.
- [17] Lin RP, Anderson KA, Ashford S, *et al.* A three-dimensional plasma and energetic particle investigation for the wind spacecraft. 1995; 71: 125-53.
- [18] Steinacker J, Miller JA. Stochastic gyroresonant electron acceleration in a low-beta plasma. I - Interaction with parallel transverse cold plasma waves. *Astrophys J* 1992; 393: 764-81.
- [19] Vainio R. Charged-particle resonance conditions and transport coefficients in slab-mode waves. *Astrophys J Suppl* 2000; 131: 519-29.

---

Received: October 27, 2008

Revised: November 26, 2008

Accepted: December 3, 2008

© Schlickeiser *et al.*; Licensee *Bentham Open*.

This is an open access article licensed under the terms of the Creative Commons Attribution Non-Commercial License (<http://creativecommons.org/licenses/by-nc/3.0/>), which permits unrestricted, non-commercial use, distribution and reproduction in any medium, provided the work is properly cited.